An overview of flux braiding experiments

Wilmot-Smith, A. L.

Published in:
Philosophical Transactions of the Royal Society A: Mathematical, Physical and Engineering Sciences

DOI:
10.1098/rsta.2014.0265

Publication date:
2015

Document Version
Publisher's PDF, also known as Version of record

PHILOSOPHICAL TRANSACTIONS A

rsta.royalsocietypublishing.org

Review

Cite this article: Wilmot-Smith AL. 2015 An overview of flux braiding experiments. *Phil. Trans. R. Soc. A* **373**: 20140265.
http://dx.doi.org/10.1098/rsta.2014.0265

Accepted: 17 November 2014

One contribution of 13 to a Theo Murphy meeting issue 'New approaches in coronal heating'.

Subject Areas:
astrophysics, mathematical physics, plasma physics

Keywords:
the Sun, corona, magnetic fields, magnetic reconnection

Author for correspondence:
A. L. Wilmot-Smith
e-mail: antonia@maths.dundee.ac.uk

An overview of flux braiding experiments

A. L. Wilmot-Smith

Division of Mathematics, Fulton Building, University of Dundee, Dundee DD1 4HN, UK

In a number of papers dating back to the 1970s, Parker has hypothesized that, in a perfectly ideal environment, complex photospheric motions acting on a continuous magnetic field will result in the formation of tangential discontinuities corresponding to singular currents. I review direct numerical simulations of the problem and find that the evidence points to a tendency for thin but finite-thickness current layers to form, with thickness exponentially decreasing in time. Given a finite resistivity, these layers will eventually become important and cause the dynamical process of energy release. Accordingly, a body of work focuses on evolution under continual boundary driving. The coronal volume evolves into a highly dynamic but statistically steady state where quantities have a temporally and spatially intermittent nature and where the Poynting flux and dissipation are decoupled on short time scales. Although magnetic braiding is found to be a promising coronal heating mechanism, much work remains to determine its true viability. Some suggestions for future study are offered.

1. Introduction

The notion that solar coronal loops are heated as an end result of magnetic braiding dates back to the 1970s and Parker's notion of topological dissipation [1–3]. The hypothesis is built on the foundation that the solar corona can be modelled as a largely force-free environment, with the Lorentz forces in force balance. However, loops themselves are subject to photospheric motions at their footpoint, and hence slow footpoint motions will lead to the quasi-static evolution of loops through sequences of force-free equilibria. Complex footpoint motions applied to the base of a coronal loop will twist

THE ROYAL SOCIETY PUBLISHING

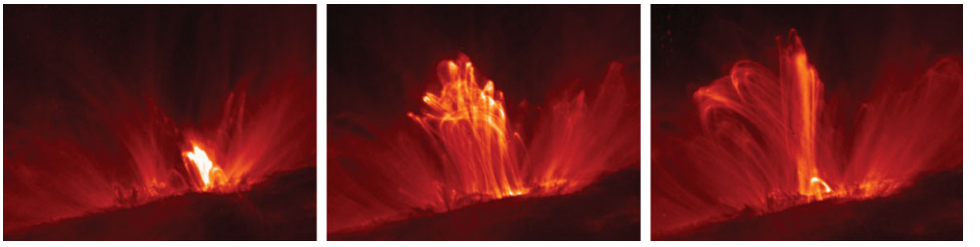

Figure 1. Evolution of an M-class solar flare observed by the *Transition Region and Coronal Explorer* (*TRACE*) at 06.34UT, 08.13UT and 09.03UT on 14 September 2000 in the 171 Å passband. An apparently tangled magnetic field structure relaxes to a simpler configuration after the flare. (Online version in colour.)

and tangle the magnetic field, which must then relax to a force-free state. Given the extremely high Lundquist numbers of the corona, the relaxation will be ideal and so will preserve exactly the magnetic field topology.

The question is then whether a magnetic field of arbitrary topology can relax ideally to a smooth force-free equilibrium. Parker hypothesized that the space of force-free fields is restricted, so that smooth equilibria will not generally exist and, instead, the magnetic field will develop tangential discontinuities corresponding to current sheets [1]. Of course, in a real corona, as soon as sufficiently small length scales develop, then diffusion will locally become appreciable and a change in the magnetic topology can occur, releasing energy. This release of magnetic energy, built up through braiding, could, under the Parker hypothesis, explain the observed high temperatures of coronal loops.

Observing braided magnetic fields in the corona has so far been fraught with difficulty. Although a very few observations (such as those of figure 1) suggest that large-scale magnetic fields can have braided configurations, most observations of coronal loops show an apparently well-combed structure. The latest high-resolution images from Hi-C are more suggestive of braids [4], although how the apparently crossing structures relate to the underlying magnetic field is not immediately clear [5]. A nonlinear force-free extrapolation of the region [6] does suggest a complex structure. Although the extrapolated magnetic field outlines the crossings seen in the observations, it is also constructed from lower-resolution magnetograms. Furthermore, the flux tube determined is split along its length, which can only be the result of at least one coronal null point. A null point in such a coronal volume is expected from our current understanding of the structure of coronal fields: they are known to be permeated by nulls, separatrix surfaces and separators [7]. A review in this volume [8] discusses the significance of heating at these features, which was already acknowledged by Parker: 'Insofar as the field is concentrated into separate individual magnetic fibrils at the photosphere, each individual fibril moves independently of its neighbours, producing tangential discontinuities (current sheets) ... There is, however, a more basic effect, viz., a continuous mapping of the footpoints spontaneously produces tangential discontinuities' [2, p. 474]. Accordingly, braiding as discussed in this review refers specifically to the elementary effect in individual elemental loops. These loops are not resolved by current instruments and, given their aspect ratio, fine-scale braiding within a loop would probably appear smoothed out.

The notion of footpoint motions acting on the complex coronal field with all of its topological features has been formalized into the theory of coronal tectonics [9]. Simulations addressing this relevant scenario are so far rare, with just a very few examining the basic effect [10–13]. One important series of articles implicitly fall into this framework [14–17]. Here, a potential magnetic field is extrapolated into the corona from a smoothed active region magnetogram and a convection-like driving velocity applied to its simulated photospheric boundary. Although the resolution of these large-scale simulations is not sufficient to provide an understanding of exactly where or how the dissipation is occurring, the broad comparisons to observed loops are encouraging.

An understanding of the viability of the Parker mechanism for coronal heating requires a two-pronged attack both by theory and by direct numerical simulation, while this review discusses only the latter approach. As I will detail in §2, numerical evidence does not, at least to date, demonstrate the ubiquitous formation of singular current sheets. Nevertheless, simulations all agree that small scales in the current do develop rapidly under generic braiding conditions and these will eventually become small enough to initiate dissipation. Hence a second main question to be tackled by braiding simulations arises: Given a finite resistivity, how does the coronal magnetic field evolve when it is continuously driven by photospheric motions? A discussion of the main simulations tackling these various questions is given in §2, presented in four broad classes according to simulation set-up. Conclusions are briefly drawn in §3 together with an outline of some suggestions for future work.

2. Braiding simulations

Numerical simulations of flux braiding naturally divide into four categories. These are not all distinct, with some simulations falling into more than one category. Nevertheless, the division is helpful to describe the present state of knowledge. In brief, the groups of simulations are:

(a) *Sequences of boundary shears*. A loop is subjected to a sequence of simple shearing motions on the boundary.
(b) *Continually driven systems*. A loop is subjected to boundary motions, generally of rotational form, for an extended period of time.
(c) *Formation of discontinuities*. The question of whether or not tangential discontinuities form in a coronal volume subjected to boundary motion is examined by simulation.
(d) *Initially braided fields*. The coronal volume is not braided self-consistently via boundary motions but a braided magnetic field is taken as an initial condition for a simulation.

All of the simulations discussed in this review have a broadly similar experimental set-up. To model the coronal loop, the magnetic field is straightened out to lie between two parallel plates. Hence a Cartesian geometry is employed and in the numerical box both the upper and lower boundaries represent the photosphere. A velocity field imposed on one or both boundaries represents a photospheric flow. The flow is two-dimensional and flux emergence (or cancellation) is not considered. I detail results found for simulations in each of the classes given above in the following sections, beginning with the earliest form of simulation, that of boundary shear.

(a) Sequences of boundary shears

Table 1 provides a short summary of simulation set-ups where initially uniform magnetic fields are subjected to shearing motions on their boundaries. Here, and throughout this section, the term 'shearing flow' is used to describe one running in opposite directions on either side of a neutral flow line. Van Ballegooijen [18,19] was the first to describe such a simulation, applying a shearing flow on the lower boundary of the domain in an alternating sequence of perpendicular directions ($\mathbf{e}_y$, $\mathbf{e}_x$, $\mathbf{e}_y$, etc.) with differing, randomly chosen, phase angles. The flow amplitude and duration were each chosen such that the maximum displacement of fluid elements on the boundary is around 16% of the domain size. The mapping of magnetic field lines from lower to upper boundary is shown to develop fine scales in the evolution, with the scales decreasing exponentially with number of shear events [18]. Although this work was developed before the concept of the quasi-separatrix layer (QSL) was developed [24], the idea is essentially the same: QSLs in the domain have a thickness exponentially decreasing in time. Fluid displacements on the upper boundary after five shears are shown in figure 2*a*.

The corresponding volume force-free magnetic field was obtained following each boundary displacement using an energy minimization iterative procedure on a 32^3 numerical grid [19]. Using this approach, a total of five shears were successfully applied before the method itself

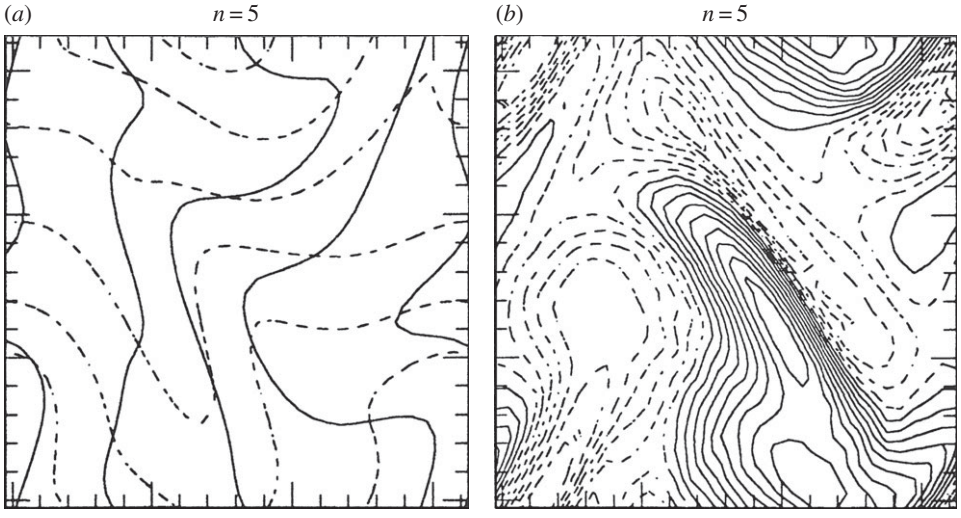

Figure 2. Illustrating the nature of the force-free equilibria attained by van Ballegooijen [19] following five boundary shearing motions applied to an initially homogeneous field. Displacement of fluid elements on the upper boundary (*a*) and vertical component of the electric current near the lower boundary (*b*). (Adapted from [19].)

Table 1. Outline of braiding simulation set-ups investigating evolution when shearing motions are applied to loops.

references	evolution method	grid size	box size	driver properties
van Ballegooijen [18,19]	magnetic energy minimization	n.a.	1^3	upper boundary only: sequence of five low-amplitude perpendicular shears with random phase angle
Mikić *et al*. [20]	simplified three-dimensional ideal MHD	64^3	1^3	lower boundary only: 12 low-amplitude perpendicular flows based on [18,19]
Longbottom *et al.* [21]	magnetofrictional	up to 65^3	1^3	fixed high-amplitude initial shear, second perpendicular shear of varying amplitude
Galsgaard & Nordlund [22]	three-dimensional resistive MHD	up to 136^3	1^3 or $1^2 \times 10$	both boundaries driven, random amplitudes, phases and durations
Bowness *et al.* [23]	three-dimensional ideal/resistive MHD	512^3	$1^2 \times 4/3$	two perpendicular shears (second switches off in one study, continues in another)

failed. While it is not *a priori* clear that the existence of small scales in the magnetic field line mapping also forces the magnetic field and current to have the same small scales, this does turn out to be the case in the example presented [19]. Hence the length scales of the current also exponentially decrease with number of shears. The current structure after five shears is shown in figure 2*b*.

Mikić *et al*. [20] took a similar approach, again applying a shear sequence to the lower boundary of a unit cube containing a magnetic field. Their numerical scheme, a simplification of the ideal magnetohydrodynamic (MHD) equations that neglects the inertial term and employs a high viscosity, allows for a successive sequence of 12 force-free relaxations on a 64^3 grid to be calculated. The main findings of van Ballegooijen [18,19] were confirmed, with the cascade

to smaller scales giving an exponential growth in current density but with a smooth force-free equilibrium achieved in each step. A consequence of the exponential decrease in current layer thickness with shear is that a tangential discontinuity will only be reached after an infinite time. However, in practice, current densities will be strong enough to become dynamically important in a plasma of finite resistivity.

While the shears applied in [18–20] all have a low amplitude (less than 20% of the domain size), Longbottom *et al.* [21] considered the question of how the shear amplitude itself (rather than number of shears) might affect the field evolution. The authors employed an ideal magnetofrictional relaxation method [25] and applied shearing motions on both the upper and lower boundaries of the domain. The initially uniform magnetic field on the unit cube was first subjected to a shear of amplitude 0.8 (as a fraction of the domain size) and then relaxed to a force-free state that was found to be smooth. This state was taken as an initial condition for a parameter study in which a perpendicular shear of various strengths was applied before relaxation. The amplitude of the second shear is shown to be crucial in determining the nature of the final force-free state. In all cases, a twisted current structure is found running through the domain. The basic structure of the twisted current layer was confirmed by Bowness *et al.* [23], who imposed analytically an initial shear and then used an ideal three-dimensional MHD code at 512^3 to evolve the magnetic field through a second, perpendicular, shear event. Taking a second shear strength of 0.5, a twisted current layer forms [23, figs 11*a* and 14] running through the domain, agreeing with [21].

The width of the current layer depends on shear strength [21]: for low shear values (below 0.5), the layer is well resolved, whereas for high shear (above 0.6), its behaviour is consistent with that of a true tangential discontinuity. That is, the maximum current in the layer increases linearly or faster as the grid resolution is increased (power-law growth is expected for a true current sheet [26]). The simulation of Longbottom *et al.* [21] marks the first (and essentially only) demonstration of a case that is consistent with Parker's scenario of topological dissipation [1]. With the resolution available at that time (a Lagrangian grid of maximum size 65^3) and known inaccuracies in the scheme for high grid deformation [27], the possibility remains that the growth of maximum current with resolution in the high-shear cases could level off at higher resolutions. An increase in grid size has only very recently become accessible [28] and this possibility is, as yet, untested.

Under either of these aforementioned scenarios (an exponential decrease in current thickness or the formation of singular current layers in ideal MHD) in a real physical plasma, the resistivity will at some point become important. To determine the consequences of a finite resistivity, Galsgaard & Nordlund [22] employed a fully resistive three-dimensional MHD simulation to examine the behaviour of a coronal loop continually subjected to boundary shearing motions. The authors detail an extensive set of simulations, common to all of which is the application of perpendicular shears of random amplitude, phase and duration to both the upper and lower boundaries of the model loop. Runs consider the effect of driver speed (0.02–0.4 compared with the Alfvén speed of 1) and duration, loop aspect ratio, and grid resolution (24^3 to 136^3), with all runs extending for many Alfvén loop crossing times.

Some results are common to each of the simulations in [22]: shearing motions cause a rapid growth in the electric current (with maximum strength increasing exponentially in the early phase), dissipation becomes important and within two or three shears a statistically steady state is reached where quantities (including the maximum current and total magnetic energy) fluctuate about an average level. In such steady states, the current structure is fragmented, with Joule dissipation taking place over a wide range of scales. Figure 3 shows isosurfaces of current in one particular run. Dissipation has an increasingly bursty character for the higher box aspect ratio cases. The magnetic field structure (some example field lines are shown in figure 3) is generally complex, including reversals in the field component perpendicular to the driven boundaries. No significant twist is built up in the system but magnetic energy in excess of potential in the steady states varies significantly. The key factor appears to be the boundary driving velocity: for the 1 : 10 aspect ratio loop, the mean energy in excess of potential in the statistically steady states is

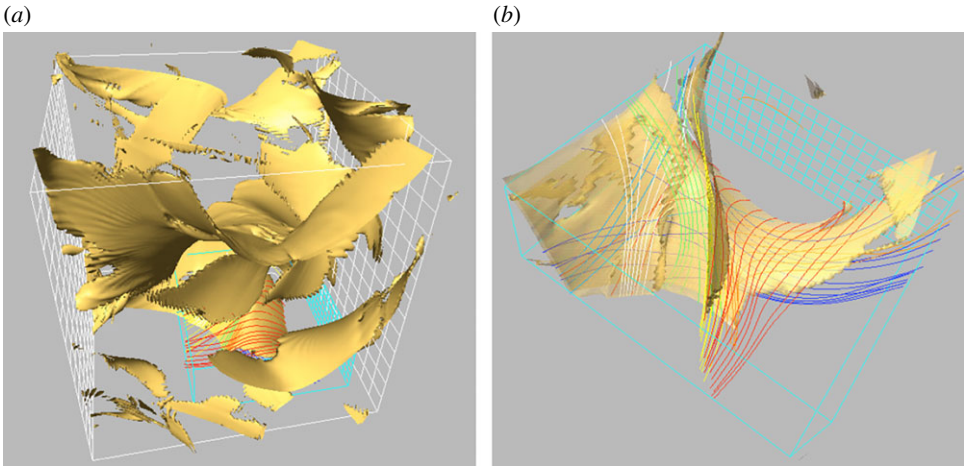

Figure 3. Instantaneous isosurfaces of current at a representative time in a simulation where a loop is continually driven by shearing boundary motions [22]. Image (*a*) shows the full domain (boundary driving surfaces indicated with a grid) and image (*b*) a subsection (the smaller blue box of image (*a*)). The current has a fully three-dimensional and space-filling structure. (Adapted from [22].) (Online version in colour.)

just 1.5% for the slower driver at a 0.02 fraction of the Alfvén velocity but 45% for the faster driver at a 0.2 fraction of the Alfvén velocity.

The simulation series of Galsgaard & Nordlund [22] is one in a wider class of simulations in which a coronal volume is continually driven under a resistive evolution. Such simulations are the subject of §2b.

(b) Continually driven systems

An outline of the continually driven simulations discussed here is given in table 2. Strong currents rapidly build up in these systems, and so in general resistive schemes are required to consider the longer-term evolution. The schemes taken vary, but a frequent choice, largely for reasons of computational efficiency, is to follow the evolution in a (resistive) reduced MHD (RMHD) scheme [38–40]. Under the RMHD assumption, an ordering to the system is assumed. The axial magnetic field component $B_0\mathbf{e}_z$ remains constant, whereas the perpendicular component $\mathbf{b}$ varies in space and time (its vector potential is evolved) and is such that $|\mathbf{b}|/B_0 \approx \epsilon \ll 1$. The velocity field is forced to be incompressible and of order ϵ, and the result is a nonlinear system of two equations that evolve the vorticity and the magnetic vector potential. The current itself is only in the vertical $\mathbf{e}_z$ direction (but depends on all three coordinates). There is typically no energy equation in an RMHD evolution, so that heat from any dissipation in the system is immediately drained away.

Of the continually driven systems outlined in table 2, two [22,23] are shearing experiments and have been described in §2a. The remaining works [29–33,36,37] have footpoint motions that are broadly similar, all being modelled on incompressible projections of convection. The convection of solar granulation is naturally compressible and allows for flux emergence and cancellation. Braiding simulations exclude these phenomena and so motivate the use of rotational cellular footpoint motions in simulations (an incompressible model for convection). Examples of such footpoint motions are illustrated in figure 4. Note that Longcope & Sudan [29] and Ng *et al.* [36] both use the same driver, which is time-dependent and derived from a source of stationary random noise (illustrated at one particular time in figure 4*b*).

In addition to the rotational drivers, Rappazzo *et al.* [34,35] present two comparison cases. These are stationary drivers, one with a constant shearing profile [34] and the other a localized

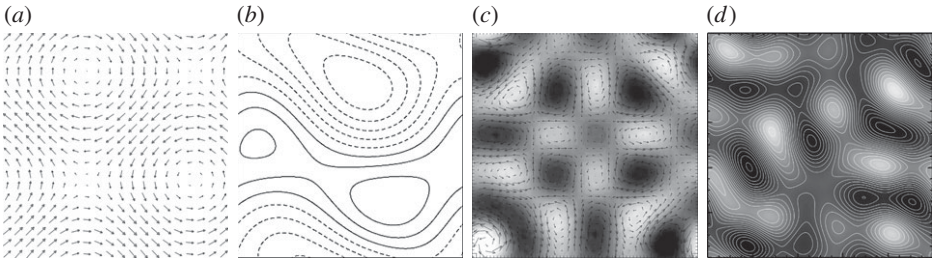

Figure 4. Streamlines and vector fields at particular times of the boundary driving velocities applied to coronal loops in various continually driven simulations. Panel (*a*) from [30] (particular frame from time-dependent simulation); panel (*b*) is a frame from the time-dependent driver of [29,36] (adapted from [41]); (*c*) from [31] (stationary driver) and (*d*) from [32,33] (stationary driver adapted from [33]).

Table 2. Outline of braiding simulation set-ups investigating continually driven coronal loops.

references	MHD evolution type	grid size	box size	driver properties
Longcope & Sudan [29]	reduced	$16^2 \times 10$ to $48^2 \times 10$	1^3	time-dependent rotational cells, both boundaries, 20–150 crossing times
Galsgaard & Nordlund [22]	resistive three dimensions	up to 136^3	1^3 and $1^2 \times 10$	time-dependent shear sequences, both boundaries, typically approximately 30 crossing times
Hendrix & van Hoven [30]	simplified three dimensions	$32^2 \times 31$ to $256^2 \times 31$	$(2\pi)^2 \times 8\pi$	time-dependent rotational cells, both boundaries, 600 crossing times
Gomez *et al.* [31]	reduced	$192^2 \times 32$, $384^2 \times 32$	$(2\pi)^2 \times 10$	stationary rotational cells, upper boundary, approximately 100 crossing times
Rappazzo *et al.* [32–35]	reduced	typically $512^2 \times 200$	$1^2 \times 10$	stationary rotational cells, both boundaries, approximately 600 crossing times [32,33] comparison cases: uniform shear [34], uniform single localized vortex [35]
Ng *et al.* [36]	reduced	$64^2 \times 16$ to $512^2 \times 64$	1^3	time-dependent rotational cells (as [29]), both boundaries, 10 000 crossing times
Dahlburg *et al.* [37]	resistive (with conduction, radiation)	128^3	$1^2 \times 5$	time-dependent rotational cells, both boundaries, 700 crossing times
Bowness *et al.* [23]	ideal and resistive three dimensions	512^3	$1^2 \times \frac{4}{3}$	two perpendicular shears, second shear indefinite or stops, both boundaries, 25 crossing times

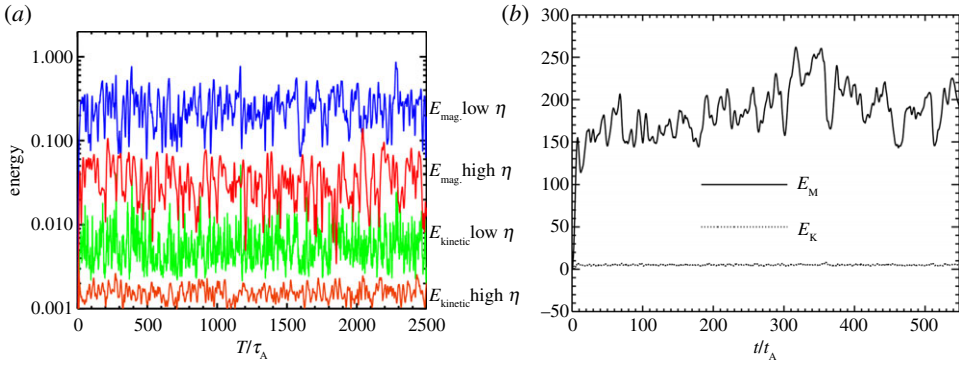

Figure 5. Variation of total magnetic and kinetic energies in time in particular simulation runs of continually driven systems: (*a*) from [36] and (*b*) from [32,33]. In both cases, time is measured in units of the Alfvén crossing time along the loop. Shown in the figures and common to all simulations of §2b is an intermittent fluctuation of the quantities about average values, with a dominance of magnetic energy over kinetic energy. (*a*) Adapted from [36]. (*b*) Adapted from [33], copyright AAS. (Online version in colour.)

single vortex motion [35]. The motivation for these simple drivers would initially be to produce instabilities (tearing mode and kink instabilities respectively) rather than as relevant profiles for field line braiding. I include these cases here to motivate a discussion of how the driver itself affects evolution.

Several features are common to each of the systems described in this section. The most fundamental feature is that, after a fairly short time, statistically steady states are reached where quantities (e.g. total magnetic and kinetic energies, dissipation) fluctuate in time about an average level. The average levels as well as the character of the intermittency both depend on the simulation details. Figure 5 shows the volume magnetic and kinetic energies in time for particular runs from [32,33,36]. In these and other cases, magnetic energy dominates significantly over kinetic energy (example ratios 10 : 1 [29], 40 : 1 [32,33,36], 80 : 1 [23]). Rappazzo *et al.* [32] find that the power spectrum of the total energy depends on the typical driving velocity compared with the Alfvén speed, steepening as the driving velocity is comparably increased (in common with [22]).

Ng *et al.* [36] show that the average free magnetic energy level increases with magnetic Reynolds number (figure 5*a*). Noteworthy for comparison is that, for the continually applied stationary shearing profile of Rappazzo *et al.* [34], a significant amount of magnetic energy initially builds up until a tearing-mode-like instability occurs. At that point, a sizable proportion of the free energy is released, but further driving leads only to a statistically steady state and no further significant free energy develops (see [34, fig. 1]). Hence, after the initial instability, the system evolution is broadly similar to those where a complex rotational braiding flow is applied. A similar finding occurs for the localized single vortex driver after the initial kink instability [35]. This suggests that the nature of the photospheric motions is not important for loop heating, in contrast to other results [42], which will be discussed in §2d.

Dissipation in these systems has a similar character, with both ohmic and viscous dissipation having a bursty, intermittent nature, illustrated for some example runs in figure 6. Poynting flux into the volume and dissipation are coupled only on long time periods, with the decorrelation being particularly notable during strong heating events [32]. The average heating rate is found to increase and the fluctuations to become increasingly fast as the magnetic Reynolds number increases [36] (see also [33, fig. 12] for example). The dependence on resistivity, η, was examined systematically first by Longcope & Sudan [29] and then over a wider range of η given the newly available increased computing power by Ng *et al.* [36]. The Ng *et al.* [36] results show that the $\eta^{-1/3}$ dependence found by Longcope & Sudan [29] begins to turn over as η is decreased. The behaviour over further orders of magnitude in η is far from clear but the data clearly warn against extrapolating the few available points to solar parameters.

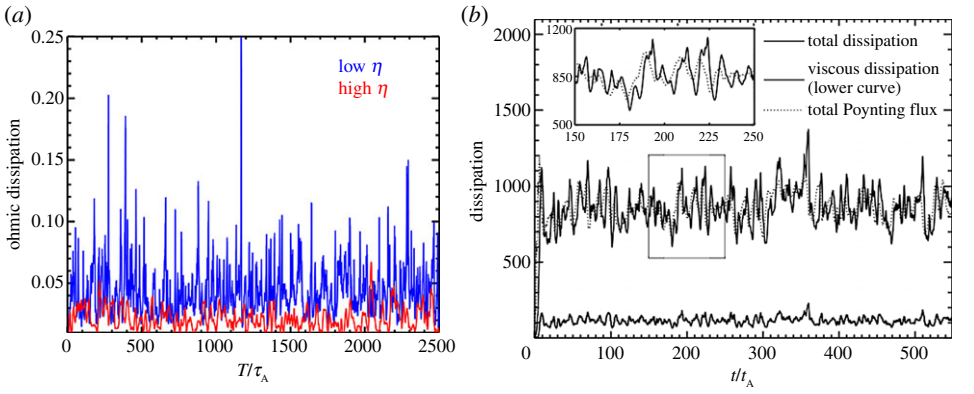

Figure 6. Dissipation shows a bursty, intermittent character in continually driven systems. (*a*) The level of dissipation increases with decreasing magnetic Reynolds number seen in the example of [36] (adapted from [36]). (*b*) Dissipation and Poynting flux balance only on long time scales but are decoupled on short periods, seen in the example of [32,33] (adapted from [32]). (Online version in colour.)

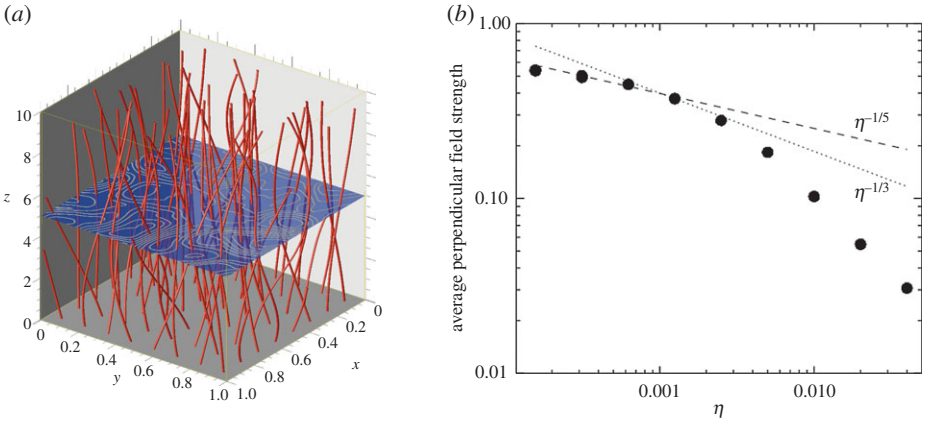

Figure 7. (*a*) Example magnetic field lines in a continually driven system of Rappazzo *et al.* [32,33] showing low levels of braiding in the statistically steady state. Adapted from [33], copyright AAS. (*b*) A detailed examination of $B_\perp$ in Ng *et al.*'s reduced MHD simulations [36] shows an increase of average $B_\perp$ as η decreases. Adapted from [36]. (Online version in colour.)

Linked with both the dissipation and the magnetic energy is the magnetic field structure. Rappazzo *et al.* [32,33] find that the magnetic field stays close to uniform, with typical inclinations being of the order of 2°, illustrated in figure 7*a*. While Rappazzo *et al.* [32,33] do not detail how the structure depends on magnetic Reynolds number, Ng *et al.* [36] examine this more closely, showing how the average perpendicular field strength $B_\perp$ increases with decreasing η (figure 7*b*). Note that a basic assumption of RMHD is that $B_\perp$ is an order of magnitude less than B_z under the evolution, and hence the findings lead one to ask whether this trend would also occur in a full three-dimensional MHD evolution.

The current structures in these continually driven systems [29–33,36,37] are broadly similar, with long thin current layers extending vertically through much of the domain (see [31, fig. 6; 33, fig. 18; 36, fig. 1] for example). Part of this structure is enforced by the basic RMHD assumption where only the vertical current component is retained. In the continually driven shearing simulations of Galsgaard & Nordlund [22], a much more fragmented and intermittent structure is found (figure 3 here, see also [22, fig. 9]). However, although a fully three-dimensional MHD evolution was considered in [22], the initial plasma beta was set at $\beta = 0.5$ and the energy

equation neglected conduction and radiation so that a high-β state developed. Note that, in the reduced MHD simulations, the lack of an energy equation essentially implies $\beta = 0$ throughout. The only fully three-dimensional MHD long-duration simulations including conduction and radiation to date seem to be those of Dahlburg *et al.* [37]. These authors are the first to show that the internal energy also has an intermittent, statistically steady nature. The temperature of their coronal loops corresponds closely to the current structure and is found to be highly spatially structured, giving a multi-thermal loop where only a fraction of the volume shows significant heating at any one time. Dahlburg *et al.* [37] find that 'the dynamics of this problem are well represented by RMHD' with low average twist (maximum 3°) and an almost incompressible flow, although a detailed comparison is not made in their letter.

(c) Formation of discontinuities

A third class of simulations consider the Parker problem, i.e. whether or not truly singular currents form under an ideal MHD evolution where a topologically simple magnetic field is subjected to complex boundary motions. Several of the sequences of boundary shear works discussed in §2a address this question. In summary, successive application of low-amplitude shear current layer thickness exponentially decreases with number of shears (i.e. finite thickness currents) [18–20]. For sufficiently strong shear, the behaviour is consistent with the formation of singular current sheets, up to the numerical resolution available [21].

Moving to the more general class of simulation, Craig & Sneyd [43] presented a series of simulations where a wide variety of boundary motions were applied to a uniform magnetic field on a unit cube, again using the magnetofrictional relaxation technique [21,25]. In almost all cases considered, smooth, well-resolved, large-scale currents are obtained. For example, following a particular combination of localized shear and compression, the current structure shown in figure 8*a* is found. Only for one type of footpoint motion do the authors find behaviour that is consistent with the formation of a singular current sheet, this being where footpoint displacements involve the side boundaries of the loop. Under these circumstances and given motions of sufficient amplitude, the maximum current in a relaxed equilibrium increases with grid resolution (to the maximum available resolution of 81^3), as illustrated in figure 8*b*. This finding is in common with Longbottom *et al.* [21]. However, the authors point out that the types of motions employed in both works are not those originally envisaged under the Parker problem (i.e. they are not complex motions internal to a loop but rather involve the entire loop).

With this in mind, a series of works by the group in Dundee have examined the nature of currents in magnetic fields that are braided [42,44–49]. The idea differs from previous simulations in that, rather than starting with a uniform magnetic field and braiding it through boundary motions, the initial configuration is already braided [44] (chosen as an analytical expression where some magnetic field lines have a pigtail braid topology while more generally field lines show a complex continuum of connectivities). Overall the configuration has no helicity, being built up from an equal number of positive and negative twists. The energy required to create the field is low, with about 3% magnetic energy in excess of potential [44]. The field line mapping of the braided magnetic field shows small scales, with the thickness of the QSLs in the field decreasing exponentially with braid complexity [45], mirroring the finding of van Ballegooijen [18] for the multiple shear case. The authors then ask whether the pigtail braid configuration can be ideally deformed to a force-free state: if so, then the space of force-free fields is surely not as restricted as Parker envisaged. To carry out this evolution, the aforementioned magnetofrictional relaxation scheme was employed [44]. The ideal relaxation is able to bring the braided field to a near-force-free state where current structures show only large scales (figure 9, left-most image). However, numerical difficulties with the scheme [27] prevent relaxation to perfectly force-free (a state that anyway can only be asymptotically reached in a simulation). A more recent detailed investigation has suggested that, as the force-free state is approached even more closely, the current structure would develop small scales, with the thickness of current layers having the same width as the QSLs of the field and so exponentially decreasing with level of braiding [49]. Again this mirrors

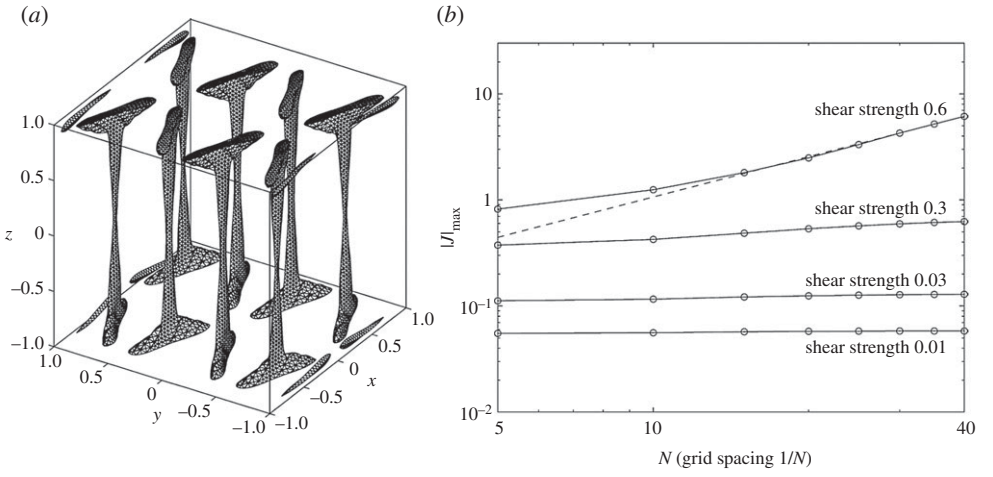

Figure 8. (*a*) Isosurfaces of current density in an equilibrium state following localized boundary motions of shear and compression applied to a uniform field and obtained under a magnetofrictional relaxation. A wide variety of boundary motions considered also resulted in smooth equilibria [43]. (*b*) Only for footpoint motions also involving the side boundaries was behaviour consistent with singular current sheet formation—illustrated by the power-law growth for sufficiently strong shear. (Adapted from [43].)

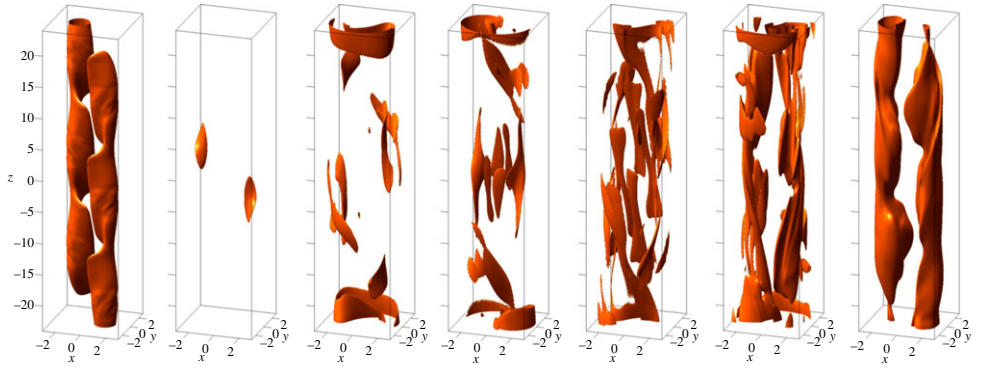

Figure 9. Isosurfaces of current in time ($t = 0, 15, 27, 35, 50, 140, 290$) during a resistive MHD relaxation of a braided magnetic field. After [47]. (Online version in colour.)

the finding of van Ballegooijen [19]. In any case, in a resistive MHD simulation, the current is found to collapse and reconnection to begin across the resulting layers [46]. The subsequent evolution of the field, together with other similar simulations, is the subject of §2d.

(d) Initially braided fields

The near-force-free magnetic field with a pigtail braid topology described in the previous section has been used as an initial condition for a resistive MHD evolution [46,47]. At the magnetic Reynolds numbers presently numerically accessible, the current system quickly intensifies and collapses to form two thin current layers [46]. These layers then fragment and a complex network of current layers with a volume-filling effect is formed (figure 9). Magnetic reconnection taking place across these layers allows the magnetic field to simplify and form an equilibrium state consisting of two unlinked flux tubes of opposite twist, associated with large-scale currents (figure 9, right-most image) [47]. Thus, although helicity is very well conserved, relaxation is

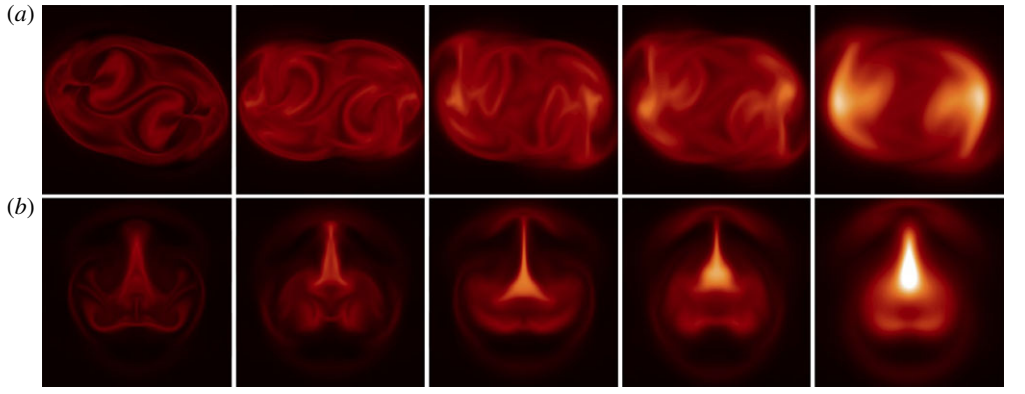

Figure 10. Loop heating in time ($t = 40, 80, 120, 180, 350$) for two contrasting resistive relaxations of braided magnetic fields. Panels show (*a*) the homogeneous heating of a complex braided field and (*b*) the more localized intense heating for a more coherently braided field. Field line averaged temperature along the loop is shown in the loop mid-plane. After [42]. (Online version in colour.)

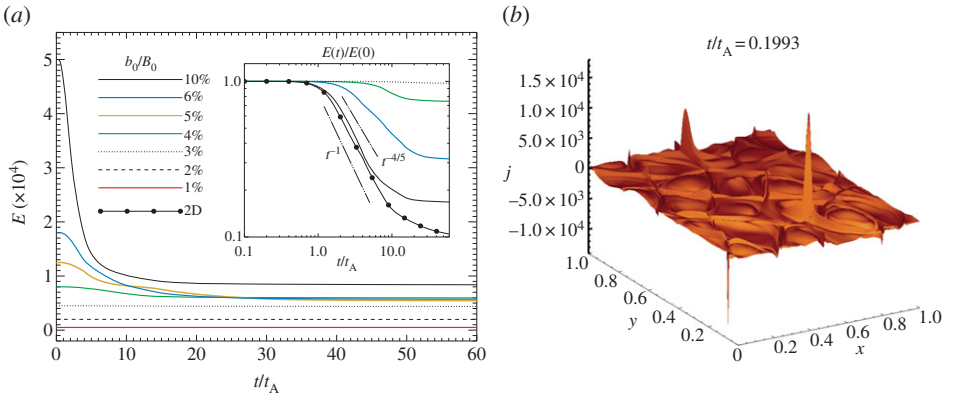

Figure 11. (*a*) Total magnetic energy in time for braided non-equilibrium magnetic fields under a resistive RMHD evolution. The ratio b_0/B_0 relates to the initial energy of the perpendicular field component. For sufficiently high b_0/B_0, a turbulent decay releases much of the free energy. (*b*) Current j_z after $t/t_A = 0.1993$ in the ideal RMHD simulation ($4096^2 \times 2048$ resolution), taken in the mid-plane of the loop. Strong and localized current layers form but it cannot be established whether or not they are singular. Adapted from [50], copyright AAS. (Online version in colour.)

not to the expected Taylor state, limiting the magnetic energy release [48]. The braiding is found to be associated with a homogeneous loop heating [42]. By contrast, a comparison case of a more coherent braided field, constructed from twisting motions of only one sign, was examined and found to lead to more localized but stronger heating [42]. These contrasting cases, illustrated in figure 10, suggest that the nature of photospheric motions will indeed have a strong impact on heating via magnetic braiding.

In a broadly similar spirit, Rappazzo & Parker [50] present a series of simulations following the resistive RMHD evolution of braided magnetic fields. The fields, not themselves in equilibrium, are constructed by superimposing a perpendicular field component made up of large-scale Fourier modes onto the background uniform field, so creating a braided loop (taken with aspect ratio 1 : 10). The loop evolution was found to depend on the ratio, b_0/B_0, between the RMS amplitude of the initial perpendicular field and the background field. For $b_0/B_0 \gtrsim 4\%$, the system develops current layers and a resistive turbulent decay ensues, with some but not all of the free

magnetic energy being dissipated (figure 11). The authors suggested that the ratio b_0/B_0 required before a violent decay could take place depends on the loop aspect ratio as approximately $l/3.5L$ (where l is the horizontal and L the vertical loop dimension). Next, Rappazzo & Parker [50] consider whether the current layers forming in the early resistive RMHD evolution would be singular in an ideal evolution. For this, the same RMHD scheme was deployed, taking a high resolution and only numerical dissipation. The analyticity strip method [51] was applied to examine whether the nature of the current evolution is indicative of a singularity, but no conclusion could be drawn, with the method itself failing. Nevertheless, the early evolution shows strong and highly localized current enhancements, as shown in figure 11*b*.

3. Conclusion and future directions

The emerging consensus from flux braiding experiments is that thin but non-singular current layers form as coronal loops are subjected to braiding motions and that the width of these layers decreases exponentially in time. With photospheric motions continually but slowly braiding the coronal volume, dissipation is an inevitable consequence. In simulations where systems have a finite resistivity and are subjected to footpoint motions over a long period of time, statistically steady states are reached where dissipation and magnetic energy fluctuate strongly in time about an average level. Although the Poynting flux into the corona must balance over a long time (with short-term decoupling present in simulations), the flux is itself dependent on the state of the coronal field. How exactly heating depends on the nature of the photospheric motions and on the coronal resistivity is not well understood.

A number of ideas arise for future attacks on the braiding problem. One is to update the simulation approach to the singularity question of Parker using improved computational techniques. For example, the magnetofrictional relaxation scheme, previously known to have numerical inaccuracies, has been significantly improved and at the same time parallelized so that simulations with an order of magnitude higher resolution are possible [28].

For the case where loops are continually subjected to boundary motions, a more detailed examination with systematic simulation set-up is required to determine what exactly are the important factors in determining the level and nature of the loop heating. Before tackling this with an RMHD approach, a careful comparison of RMHD with fully three-dimensional MHD could perhaps be fruitful.

In a move towards increased realism, a basic question is how the corona can be braided when a realistic loop is modelled. Part of this is to take a representative stratified atmosphere, with important initial advances recently presented by van Ballegooijen *et al.* [52]. Additionally, one should recall that the real corona is full of topological structure, so that how coronal fields are braided when the magnetic carpet is included, i.e. simulations addressing the coronal tectonics hypothesis [9], is another task for the near future. Similarly, along these lines, the ever-increasing computing power should allow a better resolution of large-scale simulations (e.g. [14–17]) so that their relation to braiding and coronal tectonics can be more completely established.

Acknowledgements. Helpful discussions with Peter Cargill, Jim Klimchuk and the Dundee MHD group are gratefully acknowledged.

Funding statement. This study received financial support from STFC (ST/K000993/1).

References

1. Parker EN. 1972 Topological dissipation and the small-scale fields in turbulent gases. *Astrophys. J.* **174**, 499–510. (doi:10.1086/151512)
2. Parker EN. 1988 Nanoflares and the solar X-ray corona. *Astrophys. J.* **330**, 474–479. (doi:10.1086/166485)
3. Parker EN. 1994 *Spontaneous current sheets in magnetic fields: with applications to stellar X-rays*. International Series in Astronomy and Astrophysics. Oxford, UK: Oxford University Press.

4. Cirtain JW, *et al.* 2013 Energy release in the solar corona from spatially resolved magnetic braids. *Nature* **493**, 501–503. (doi:10.1038/nature11772)
5. Cargill P. 2013 Solar physics: towards ever smaller length scales. *Nature* **493**, 485–486. (doi:10.1038/493485a)
6. Thalmann JK, Tiwari SK, Wiegelmann T. 2014 Force-free field modeling of twist and braiding-induced magnetic energy in an active region corona. *Astrophys. J.* **780**, 102. (doi:10.1088/0004-637X/780/1/102)
7. Priest ER. 2014 *Magnetohydrodynamics of the Sun*. Cambridge, UK: Cambridge University Press.
8. Parnell CE, Stevenson JEH, Threlfall J, Edwards SJ. 2015 Is magnetic topology important for heating the solar atmosphere? *Phil. Trans. R. Soc. A* **373**, 20140264. (doi:10.1098/rsta.2014.0264)
9. Priest ER, Heyvaerts JF, Title AM. 2002 A flux-tube tectonics model for solar coronal heating driven by the magnetic carpet. *Astrophys. J.* **576**, 533–551. (doi:10.1086/341539)
10. Mellow C, Gerrard CL, Galsgaard K, Hood AW, Priest ER. 2005 Numerical simulations of the flux tube tectonics model for coronal heating. *Solar Phys.* **227**, 39–60. (doi:10.1007/s11207-005-1713-2)
11. De Moortel I, Galsgaard K. 2006 Numerical modelling of 3D reconnection due to rotational footpoint motions. *Astron. Astrophys.* **451**, 1101–1115. (doi:10.1051/0004-6361:20054587)
12. De Moortel I, Galsgaard K. 2006 Numerical modelling of 3D reconnection II. Comparison between rotational and spinning footpoint motions. *Astron. Astrophys.* **459**, 627–639. (doi:10.1051/0004-6361:20065716)
13. Wilmot-Smith AL, De Moortel I. 2007 Magnetic reconnection in flux tubes undergoing spinning footpoint motions. *Astron. Astrophys.* **473**, 615–623. (doi:10.1051/0004-6361:20077455)
14. Gudiksen BV, Nordlund Å. 2002 Bulk heating and slender magnetic loops in the solar corona. *Astrophys. J.* **572**, L113–L116. (doi:10.1086/341600)
15. Peter H, Gudiksen BV, Nordlund Å. 2004 Coronal heating through braiding of magnetic field lines. *Astrophys. J.* **617**, L85–L88. (doi:10.1086/427168)
16. Gudiksen BV, Nordlund Å. 2005 An *ab initio* approach to the coronal heating problem. *Astrophys. J.* **618**, 1020–1030. (doi:10.1086/426063)
17. Gudiksen BV, Nordlund Å. 2005 An *ab initio* approach to solar coronal loops. *Astrophys. J.* **618**, 1031–1038. (doi:10.1086/426064)
18. van Ballegooijen AA. 1988 Force free fields and coronal heating Part 1. The formation of current sheets. *Geophys. Astrophys. Fluid Dyn.* **41**, 181–211. (doi:10.1080/03091928808208850)
19. van Ballegooijen AA. 1988 Magnetic fine structure of solar coronal loops. In *Solar and stellar coronal structure and dynamics*. *Proc. Ninth Sacramento Peak Summer Symp., Sunspot, NM*, pp. 115–124. Sunspot, NM: National Solar Observatory.
20. Mikić Z, Schnack DD, van Hoven G. 1989 Creation of current filaments in the solar corona. *Astrophys. J.* **338**, 1148–1157. (doi:10.1086/167265)
21. Longbottom AW, Rickard GJ, Craig IJD, Sneyd AD. 1998 Magnetic flux braiding: force-free equilibria and current sheets. *Astrophys. J.* **500**, 471–482. (doi:10.1086/305694)
22. Galsgaard K, Nordlund Å. 1996 Heating and activity of the solar corona 1. Boundary shearing of an initially homogeneous magnetic field. *J. Geophys. Res.* **101**, 13445–13460. (doi:10.1029/96JA00428)
23. Bowness R, Hood AW, Parnell CE. 2013 Coronal heating and nanoflares: current sheet formation and heating. *Astron. Astrophys.* **560**, A89. (doi:10.1051/0004-6361/201116652)
24. Titov VS, Hornig G, Démoulin P. 2002 Theory of magnetic connectivity in the solar corona. *J. Geophys. Res.* **107**, 1164. (doi:10.1029/2001JA000278)
25. Craig IJD, Sneyd AD. 1986 A dynamic relaxation technique for determining the structure and stability of coronal magnetic fields. *Astrophys. J.* **311**, 451–459. (doi:10.1086/164785)
26. Ali F, Sneyd A. 2001 Magnetic equilibria resulting from a helically symmetric kink instability. *Geophys. Astrophys. Fluid Dyn.* **94**, 221–248. (doi:10.1080/03091920108203408)
27. Pontin DI, Hornig G, Wilmot-Smith AL, Craig IJD. 2009 Lagrangian relaxation schemes for calculating force-free magnetic fields, and their limitations. *Astrophys. J.* **700**, 1449–1455. (doi:10.1088/0004-637X/700/2/1449)
28. Candelaresi S, Pontin D, Hornig G. 2014 Mimetic methods for Lagrangian relaxation of magnetic fields. *SIAM J. Sci. Comput.* **36**, B952–B968. (doi:10.1137/140967404)
29. Longcope DW, Sudan RN. 1994 Evolution and statistics of current sheets in coronal magnetic loops. *Astrophys. J.* **437**, 491–504. (doi:10.1086/175013)
30. Hendrix DL, van Hoven G. 1996 Magnetohydrodynamic turbulence and implications for solar coronal heating. *Astrophys. J.* **467**, 887–893. (doi:10.1086/177663)

31. Gomez DO, Dmitruk PA, Milano LJ 2000. Recent theoretical results on coronal heating. *Solar Phys.* **195**, 299–318. doi:10.1023/A:1005283923956
32. Rappazzo AF, Velli M, Einaudi G, Dahlburg RB. 2007 Coronal heating, weak MHD turbulence, and scaling laws. *Astrophys. J.* **657**, L47–L51. (doi:10.1086/512975)
33. Rappazzo AF, Velli M, Einaudi G, Dahlburg RB. 2008 Nonlinear dynamics of the Parker scenario for coronal heating. *Astrophys. J.* **677**, 1348–1366. (doi:10.1086/528786)
34. Rappazzo AF, Velli M, Einaudi G. 2010 Shear photospheric forcing and the origin of turbulence in coronal loops. *Astrophys. J.* **722**, 65–78. (doi:10.1088/0004-637X/722/1/65)
35. Rappazzo AF, Velli M, Einaudi G. 2013 Field lines twisting in a noisy corona: implications for energy storage and release, and initiation of solar eruptions. *Astrophys. J.* **771**, 76. (doi:10.1088/0004-637X/771/2/76)
36. Ng CS, Lin L, Bhattacharjee A. 2012 High-Lundquist number scaling in three-dimensional simulations of Parker's model of coronal heating. *Astrophys. J.* **747** 109. (doi:10.1088/0004-637X/747/2/109)
37. Dahlburg RB, Einaudi G, Rappazzo AF, Velli M. 2012 Turbulent coronal heating mechanisms: coupling of dynamics and thermodynamics. *Astron. Astrophys.* **544**, L20. (doi:10.1051/0004-6361/201219752)
38. Stauss HR. 1976 Nonlinear, three-dimensional magnetohydrodynamics of noncircular tokamaks. *Phys. Fluids* **19**, 134–140. (doi:10.1063/1.861310)
39. Stauss HR. 1977 Dynamics of high beta tokamaks. *Phys. Fluids* **20**, 1354–1360. (doi:10.1063/1.862018)
40. Rosenbluth MN, Monticello DA, Strauss HR, White RB. 1976 Numerical studies of nonlinear evolution of kink modes in tokamaks. *Phys. Fluids* **19**, 1987–1996. (doi:10.1063/1.861430)
41. Longcope DW. 1993 Theoretical studies of magnetohydrodynamic equilibria and dynamics of a solar coronal loop. PhD thesis, Cornell University, Ithaca, NY, USA.
42. Wilmot-Smith AL, Pontin DI, Yeates AR, Hornig G. 2011 Heating of braided coronal loops. *Astron. Astrophys.* **536**, A67. (doi:10.1051/0004-6361/201117942)
43. Craig IJD, Sneyd AD. 2005 The Parker problem and the theory of coronal heating. *Solar Phys.* **232**, 41–62. (doi:10.1007/s11207-005-1582-8)
44. Wilmot-Smith AL, Hornig G, Pontin DI. 2009 Magnetic braiding and parallel electric fields. *Astrophys. J.* **696**, 1339–1347. (doi:10.1088/0004-637X/696/2/1339)
45. Wilmot-Smith AL, Hornig G, Pontin DI. 2009 Magnetic braiding and quasi-separatrix layers. *Astrophys. J.* **704**, 1288–1295. (doi:10.1088/0004-637X/704/2/1288)
46. Wilmot-Smith AL, Pontin DI, Hornig G. 2010 Dynamics of braided coronal loops. I. Onset of magnetic reconnection. *Astron. Astrophys.* **516**, A5. (doi:10.1051/0004-6361/201014041)
47. Pontin DI, Wilmot-Smith AL, Hornig G, Galsgaard K. 2010 Dynamics of braided coronal loops. II. Cascade to multiple small-scale reconnection events. *Astron. Astrophys.* **525**, A57. (doi:10.1051/0004-6361/201014544)
48. Yeates AR, Hornig G, Wilmot-Smith AL. 2010 Topological constraints on magnetic relaxation. *Phys. Rev. Lett.* **105**, 085002. (doi:10.1103/PhysRevLett.105.085002)
49. Pontin DI. In preparation. On the degree of field line braiding in coronal loops.
50. Rappazzo AF, Parker EN. 2013 Current sheets formation in tangled coronal magnetic fields. *Astrophys. J.* **773**, L2. (doi:10.1088/2041-8205/773/1/L2)
51. Sulem C, Sulem P-L, Frisch H. 1983 Tracing complex singularities with spectral methods. *J. Comput. Phys.* **50**, 138–161. (doi:10.1016/0021-9991(83)90045-1)
52. van Ballegooijen AA, Asgari-Targhi M, Berger MA. 2014 On the relationship between photospheric footpoint motions and coronal heating in solar active regions. *Astrophys. J.* **787**, 87. (doi:10.1088/0004-637X/787/1/87)